ESR and magnetization of the spin-glass *Cu*Mn at low concentrations

F. R. Hoekstra and G. J. Nieuwenhuys
Kamerlingh Onnes Laboratorium der Rijksuniversiteit Leiden, 2300 RA Leiden, the Netherlands

K. Baberschke
Institut für Atom- und Festkörperphysik der Freien Universität Berlin, D-1000 Berlin 33, West Germany

S. E. Barnes
Physics Department, University of Miami, Coral Gables, Florida 33124
(Received 13 May 1983)

We have determined the resonance frequency ω versus resonant field H diagram for *Cu*Mn with Mn concentrations 2, 3.5, and 5 at. %, both when $\vec{H}$ is parallel and antiparallel to the cooling field $\vec{H}_c$. From the parallel measurements we find anisotropy energy density constants K that are in agreement with K values determined from transverse susceptibility and torque measurements. However, the K values determined from the remanence reversal of dc magnetization are smaller by a factor of approximately 2. We suggest that this is caused by a breakdown of rigid-body spin rotations. By combining the parallel data with the antiparallel data, we obtain sets of K values for the vector model and the triad model which are unphysical. We attribute this also to nonrigid spin rotations. In addition, we present the full angle dependence of ESR measurements for the 5-at. % sample, which shows that the quantitative agreement with the two models breaks down when the angle θ_R between $\vec{\sigma}$ and $\vec{H}_c$ is greater than $\approx 25°$ for this concentration. Finally, we have carefully searched for the predicted ω^- mode in small external fields, but we have not observed it. By using the concept of oscillator strength we proceed to calculate this effect for the vector anisotropy model. We find the ESR intensity of the expected ω^- mode to be $\approx 1\%$ of that of the ω^+ mode. Nevertheless, under our experimental conditions this should not preclude its observation.

I. INTRODUCTION

Two hydrodynamic models have been proposed to explain the ESR of spin-glasses. The vector model[1] uses an anisotropy energy density K that is connected with a preferred direction, given by the unit vector $\hat{N}$. This direction is not in any way connected with the crystalline axes,[2] but instead it is induced by field-cooling the sample from $T \gg T_f$ (the freezing temperature) to $T \ll T_f$ in a cooling field $\vec{H}_c$ along a certain direction. Using the vector model one can calculate the equilibrium direction, given by the unit vector $\hat{n}$, of the remanence $\vec{\sigma}$, if, after the field cooling, the field $\vec{H}_c$ is taken away and another field $\vec{H}$ is applied in an arbitrary direction, specified by θ_H (the angle between $\vec{H}$ and $\vec{H}_c$). Then, for small oscillations of the total magnetization $\vec{M}$ (composed of the rotated remanence $\vec{\sigma}$ and an isotropic magnetization $\chi_{\rm iso}\vec{H}$) about its equilibrium direction, the resonant frequencies can be calculated. In this paper, we shall extend the vector model by calculating the oscillator strength of the resonant modes which are predicted. In contrast, the triad model[3,4] claims that the anisotropy energy is determined by the orientation of a spin triad $\hat{h},\hat{p},\hat{q}$, relative to a reference triad $\hat{N},\hat{P},\hat{Q}$.[5] We shall take $\hat{N}||\vec{H}_c$. Also in this model the resonance frequencies have been calculated. The most striking difference between the two models is the prediction, in the triad model, of an additional, longitudinal resonance mode ω_L. However, in the case when the remanence $\vec{\sigma}$ remains in the original direction $\hat{N}$, the predictions of both models are the same for the other two modes, labeled ω^+ and ω^-. Several recent publications indicate that it is the triad model which is best able to describe the measurements.[6,7]

In Sec. II we present a description of our measurements. The experimental results, described in Sec. III, are divided in two parts. Firstly, we have measured the resonant frequency ω versus the resonant field H at 4 frequencies, namely 1.122, 3.44, 4.03, and 9.53 GHz, both when $\vec{H}$ is parallel and antiparallel to $\vec{H}_c$, for spherical samples of *Cu*Mn(x at. %) with $x=2$, 3.5, and 5. Secondly, we exhibit the full angle dependence of the ESR for *Cu*Mn(5 at. %) at 9.4 GHz.

In order to explain why we do not observe the predicted ω^- mode (nor do we observe the triad model's ω_L mode), we calculate the oscillator strength of ω^+ and ω^- modes in the vector model. Our calculations, presented in Sec. IV, yield an expected ESR peak-to-peak amplitude for the ω^- mode which is $\approx 1\%$ of that which is predicted for the ω^+ mode. In view of the fact that all our *Cu*Mn ω^+ resonances are very strong indeed, we feel that we have enough experimental sensitivity to observe lines that would be 100 times weaker. Therefore, the oscillator strength alone may not be sufficient and other considerations will have to come into play. We summarize our conclusions in Sec. V.

II. EXPERIMENTAL DESCRIPTION

The ESR experiments were performed using homodyne reflection spectrometers and commercial gas-flow cryostats where the temperature was determined by thermocouples at the sample site. The field-cooled (FC) spectra were obtained after cooling the samples from $T > 2T_f$ to $T \ll T_f$ in a field H_c.[8] After cooling we recorded the resonance with decreasing field. The magnetization M which is measured with decreasing field is slightly larger than that measured subsequently with an increasing field. This small hysteresis in M leads to a small hysteresis in the ESR, as was demonstrated in Fig. 2 of Ref. 9.

For the zero-field-cooled (ZFC) spectra the remanent field of the magnet was not larger than 60 G.[10] The shift S of the resonance line is determined with respect to $g=2$. For fixed temperature T, S is smallest for samples cooled in our largest attainable field H_c of 12 kG. As the cooling field decreases, the shift increases, in agreement with the H_c dependence of σ.

ESR data were obtained at four frequencies, namely 1.122, 3.44, 4.03, and 9.53 GHz, always for spherical samples. The magnetization of the identical samples was measured in a Foner vibrating-sample magnetometer. Care was taken to repeat exactly the same FC and T cycles that were used in the ESR.

The samples were made by melting together the constituent elements in the appropriate amounts. No significant difference was detected between samples that had been arc-melted and samples made in a high-frequency induction furnace and subsequently quenched. Of the samples used in the present investigation, the 2- and 5-at.% concentrations were measured both in ESR and in dc magnetization, as obtained from the melt. Only the 3.5-at.% sample obtained an additional anneal of 16 h at 800 °C before any data were taken. Then, after the bulk of the measurements herein described had been completed, we checked some additional metallurgical aspects for the 5-at.% concentration: A number of samples were formed into spheres and cylinders by spark-cutting. At X band no difference was seen between these spheres and cylinders. Next, we deformed part of the original material by cold-rolling until there had been a 20% reduction in thickness; we also made spheres and cylinders from this material. Again, there was no difference between these samples and the series that had not been cold-worked, either in the FC spectra or the ZFC spectra. Subsequently, we checked the influence of a 1-h strain-relieving anneal in dynamical vacuum at 450 °C. No change occurred in the resonance properties.

Finally, a number of samples were subjected to a homogenizing anneal at 800 °C for 16 h. After this anneal, there were indeed some changes; most notably in the ZFC spectra, where the field for resonance shifted down by values between 200 and 400 G. Since we do not consider ZFC in the present report, this has no influence on our conclusions.

All samples were heavily etched in HNO_3 immediately prior to measurement. When we measured samples that had been left exposed to the air for some days, we found that the resonance lines at low temperatures were deformed, but, what is even more serious, the lines both in FC and ZFC were shifted towards $g=2$. We are convinced that these effects are due to surface contamination, especially as etching of the samples always brings back the original lines. We have therefore been most careful to avoid any such contamination.

III. EXPERIMENTAL RESULTS

A. ω vs H at $\theta_R = 0$

We have determined the resonant field H as a function of the cooling field H_c at four spectrometer frequencies for the three concentrations, always at our lowest temperature, ≈ 3 K. On the right-hand sides of Figs. 1–3 we show these data for the three concentrations. In order not to clutter the figures with data points, we only show those points for which $H_c = 12$ kG (H is parallel to H_c). Now we want to compare these data with the predictions of the hydrodynamic theory. In this limit of parallel $\vec{H}$ and $\vec{H}_c$ the theories agree on the formula,

$$\left[\frac{\omega}{\gamma}\right]^{\pm} = \left[\frac{H}{2} - \frac{\sigma}{2\chi}\right] \pm \left[\left[\frac{H}{2} + \frac{\sigma}{2\chi}\right]^2 + \frac{K^+}{\chi}\right]^{1/2}, \quad (1)$$

for the ω^+ and ω^- modes.

We determined the σ and χ values that are needed from dc-magnetization measurements in which we used exactly the same FC and T cycles that we used in the ESR. Only K^+ is left as an unknown parameter now.

There are two ways to determine K^+. In the first place, one can use the fact that the models which predict the ESR modes also make predictions for the magnetization behavior (as already indicated in the Introduction). If the total anisotropy energy density is composed of unidirectional anisotropy K_1 and uniaxial anisotropy K_2, then displaced square hysteresis curves should be found (at $T=0$) centered at $H_M = -K_1/\sigma$ with a total width $\Delta H = 2K_2/\sigma$ (cf. columns 4 and 5 of Table I); so that the reversal from $\vec{\sigma}$ parallel to $\hat{N}$ ($\theta_R = 0$) to $\vec{\sigma}$ antiparallel to $\hat{N}$ ($\theta_R = \pi$) should take place at $H_\downarrow = -(K_1+K_2)/\sigma \equiv -K^+/\sigma$. Obviously, a simple measurement of $H_\downarrow$ and σ yields K^+, which is exactly the quantity that we need. However, it has been clearly established by various authors that this way of determining K^+ is not the right one. The reason for this is that in calculating H_M, ΔH, $H_\downarrow$, etc., there is the implicit assumption in the models that $|\vec{\sigma}|$ is invariant during the reversal, which means that it is supposed that the vector $\vec{\sigma}$ actually retains its modulus while making a rotation by π in a plane perpendicular to some unspecified axis. It turns out that this is not what really happens. What happens is probably that the remanences $\vec{\sigma}_i$ of the individual clusters in the spin-glass each rotate by π along individual axes which are completely randomly oriented in the plane perpendicular to $\vec{H}$.

Most authors have found that the K values determined

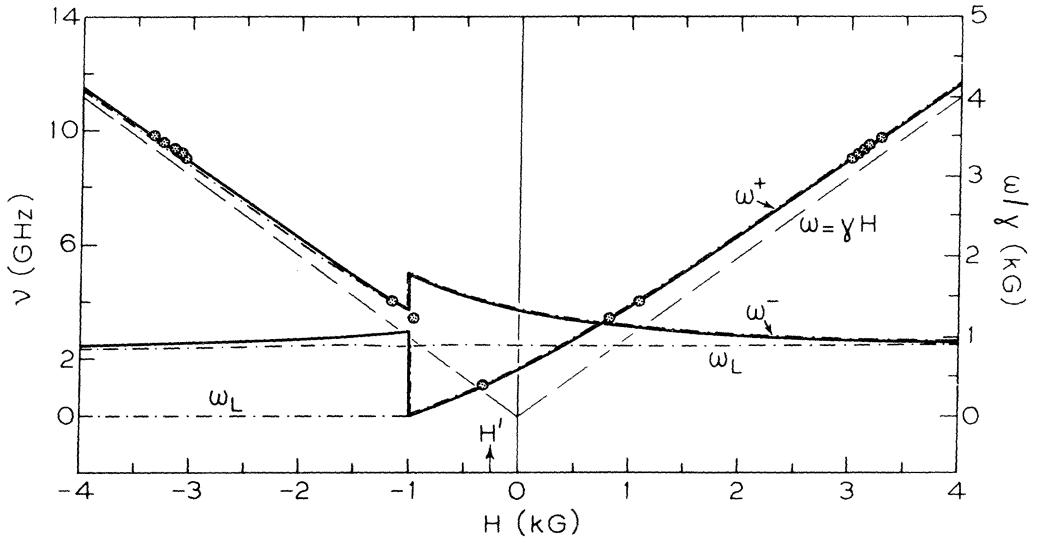

FIG. 1. ω/γ-vs-H diagram for CuMn(2 at. %) sphere at $T\approx 3$ K ($T_f=17$ K). The right-hand side of the diagram corresponds to $\vec{H}\|\vec{H}_c$ ($\theta_H=0$), and the left-hand side corresponds to $\vec{H}$ antiparallel to $\vec{H}_c(\theta_H=\pi)$. Dot-filled circles represent data points for which $H_c=12$ kG. Solid lines are theoretical mode predictions in the vector model, and dashed-dotted lines are for the triad model. Note that for $H>-1$ kG, which is where $\vec{\sigma}$ should reverse given K^+ and $|\vec{\sigma}|$, triad-model predictions for ω^+ and ω^- are the same as in the vector model. Actual $\vec{\sigma}$ jump takes place at smaller negative field H' (see arrow). For convenience, ω/γ has also been plotted in terms of spectrometer frequency ν in GHz. Conversion is via $\omega/\gamma=(h/2\mu_B)\nu$.

from transverse susceptibility and low-angle torque measurements, where the implicit assumptions of the model *do* hold, are larger, by a factor of approximately 2, than K values determined from the remanence reversal.[11] We feel that this factor of 2 is not completely coincidental, but, instead, corresponds to some geometrical average of anisotropy energies of the individual clusters for π rotations.

The second way of determining K^+ is to make the assumption that in the ESR measurements, where the angular deviations from $\theta_R=0$ are very small (considering that the microwave field $h\lesssim 0.1$ G, whereas the measuring field H is at least several hundred gauss, and the anisotropy field, as we shall see below, is at least 1000 G), it is also the "real" K^+ which manifests itself. This is equivalent to saying, for these small rotations away from equilibrium, that the spin system behaves as a rigid body, whose macroscopic remanence $\vec{\sigma}$ is linked to its memory direction $\hat{N}$ by a well-defined anisotropy energy density K^+.

We have determined K^+ from the ESR itself using the formula

$$K^+=[(\omega/\gamma)-H^0][\chi(\omega/\gamma)+\sigma]\ , \tag{2}$$

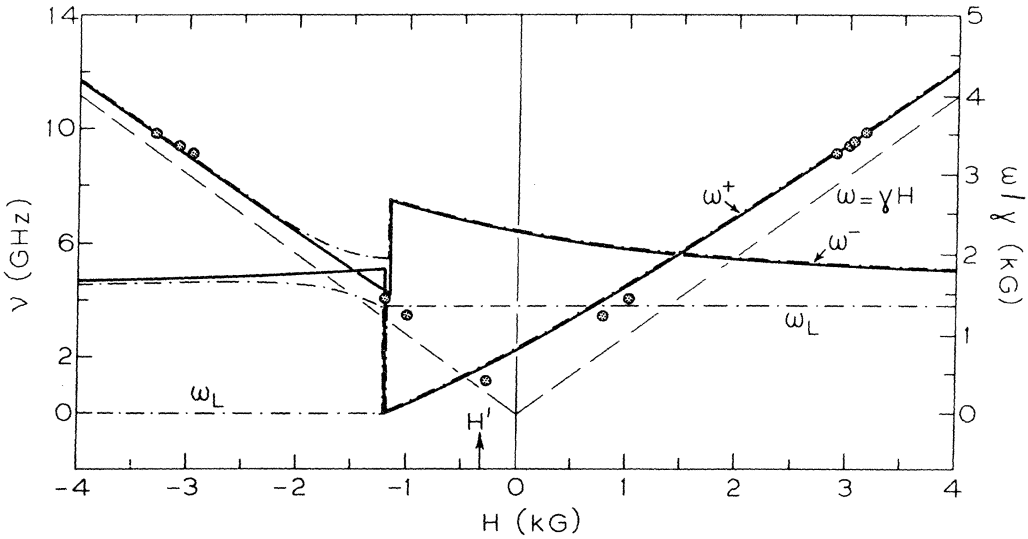

FIG. 2. ω/γ-vs-H diagram for CuMn(3.5 at. %) sphere at $T\approx 3$ K ($T_f=22$ K). Details as in Fig. 1. Frequency for which theory has been fitted to data is 9.853 GHz, which accounts for rather larger deviations between theory and experiment at 4, 3, and 1 GHz. Data point at $\nu=3.44$ GHz and $H=-1$ kG is not on predicted mode line because the theory predicts that $\vec{\sigma}$ has not reversed yet, whereas actual reversion has already taken place at field H' shown with arrow.

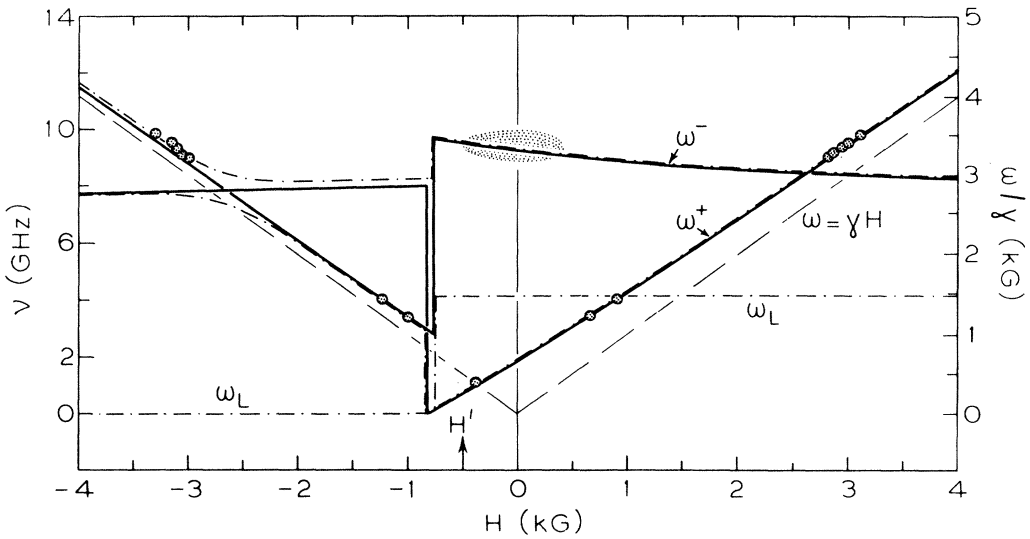

FIG. 3. ω/γ-vs-H diagram for *Cu*Mn(5 at. %) sphere at $T\approx 3$ K ($T_f=29$ K). Details as in Figs. 1 and 2. Also shown is the region where we have searched for the predicted ω^- mode. See Sec. IV.

which can easily be obtained from Eq. (1).[1] Here, H^0 is the resonance field for $\theta_R=0$; the formula is valid for the ω^+ mode. Comparing K^+ values for various cooling fields at fixed frequency and concentration, there is a fluctuation of at most 10%. K values obtained for various frequencies at constant concentration and cooling field are constant to within 20%. At 3 K, independent of frequency *or* cooling field, we find $K^+=ac_{\mathrm{Mn}}^2$ with $a=(130\pm 20)$ erg/cm^3(at. %)^2.

Indeed we find that K^+ values thus determined are approximately 2 times larger than those we find from dc-magnetization reversal. Also, our K^+ values, as well as the c_{Mn}^2 dependence of K^+, show excellent quantitative agreement with values quoted by other authors for similar samples under similar conditions.[12]

In Figs. 1–3 we have plotted, by thin solid lines, the function expressed in Eq. (1); however, instead of using an averaged K^+, we take a value for K^+ determined from one data point at a reference frequency. In this way, one gets a better impression of the deviations between the data points and the formula. So far all data points have been identified as ω^+ resonances. No ω^- resonances have been seen in our experiments. An ω^- resonance has been reported once.[1] (The ω_L mode cannot be detected in a conventional fixed-frequency experiment except through admixture of ω_L in one of the transverse modes.[7]) We shall come back to this point in Sec. IV.

We now turn to the resonance behavior in the case where $\vec{\sigma}$ is antiparallel to $\vec{\mathrm{H}}_c$ ($\theta_R=\pi$). We have plotted the measured points on the left-hand sides of Figs. 1–3. Now we also want to compare the theoretical ω-vs-H descriptions for this side of the diagram. At first glance, one might be tempted to use Eq. (1) with negative values for H, and, after the reversal of $\vec{\sigma}$, also a negative value for σ. This, however, is not the correct procedure. We found this by calculating the full angle-dependent $\omega(H)$ relationship from the vector-model free energy of Ref. 1; for the triad model we used the corresponding relationship, Eq. (4.3), from Ref. 3. It turns out that in the limit $\theta_H=\pi$ but $\theta_R=0$ (the field H is negative but the remanence σ has not reversed yet), we are still permitted to use an extrapolation from the ω-vs-H diagram with $\theta_H=\theta_R=0$. However, once $\vec{\sigma}$ *has* reversed, the new relationship between ω and H can only be obtained from the original one at $\theta_H=0$, if, not only H and σ, but also K, is given a negative sign. This means that if one plots the theoretical mode prediction, either in the vector or the triad model, using the previously obtained (positive) value for K^+, there is no correspondence with measured data points. We have done the following: In the triad theory it is shown that the effective anisotropy energy density is in fact angle dependent via $K=\tilde{K}(\theta_R)\cos\theta_R$, where $\tilde{K}(\theta_R)=K_1+K_2\cos\theta_R$, which means that $K^+=\tilde{K}(\theta_R=0)=K_1+K_2$ and $K^-=\tilde{K}(\theta_R=\pi)=K_1-K_2$. We have calculated a value for K^- at one fixed point where $\theta_R=\pi$, both in the vector model and in the triad model. In the vector model,

$$K^-=[H^\pi-(\omega/\gamma)][\chi(\omega/\gamma)+\sigma]\,, \tag{3}$$

where H^π is the resonance field at $\theta_R=\pi$ (all quantities H^π, ω, χ, and σ *are positive numbers),* and in the triad model,

$$K^-=\chi\frac{-(\omega/\gamma)^4+(\omega/\gamma)^2(H^{\pi 2}+H_R^2)-H^{\pi 2}H_R^2}{(\omega/\gamma)^2-H^\pi H_R}\,, \tag{4}$$

where $H_R=\sigma/\chi$. With the value of K^- determined from one data point at a reference frequency, and the value of K^+ that we already had (at the same frequency), we now calculate values of K_1 and K_2 using $K_1=\frac{1}{2}(K^++K^-)$ and $K_2=\frac{1}{2}(K^+-K^-)$.

The theory is then tested if all data points at $\theta_R=\pi$ can be fitted (approximately) with these values of K_1 and K_2, and, of course, if the K_1 and K_2 values are physical. In Figs. 1–3 we show, on the left-hand sides, the theoretical predictions in the vector model (again using thin solid

TABLE I. Comparison between magnetization data and ESR data for *Cu*Mn(x at. %). Figures for K_1 and K_2 for the ESR vector and triad model, result from $\theta_H=0$ and π fits (see Figs. 1–3). In Sec. III we argue that those fits are unphysical (cf. Fig. 4). The last column lists the ESR K^+ value that is found for $\theta_H=0$; we attribute this to a unidirectional anisotropy.

		Magnetization				ESR (vector model)			ESR (triad model)		
x (at.%)	σ (G)	χ (10^{-4})	K_1 (erg/cm^3)	K_2 (erg/cm^3)	K_1+K_2 (erg/cm^3)	K_1 (erg/cm^3)	K_2 (erg/cm^3)	K_1 (erg/cm^3)	K_2 (erg/cm^3)	ESR $K^+=K_1+K_2$ (erg/cm^3)
2	0.46	6.1	0	115	115	47	421	−44	513	468
3.5	1.57	10.6	290	235	525	424	1484	−35	1943	1908
5	3.54	13.4	1221	531	1752	908	2001	−10	2920	2909

lines) and in the triad model (using dashed-dotted lines). At the reference frequencies [4.03 GHz for 2 and 5 at. %, and 9.853 GHz for 3.5 at. % (Ref. 13)] the predictions necessarily agree with the data points. In Table I we have collected the data obtained so far and we also show the values found for K_1 and K_2. The vector model yields $K_1 \ll K_2$, contradicting the magnetization data. In the triad model one even needs negative K_1 values, which are obviously unphysical. From our four frequencies, and for a given K, we are not able to verify any mode splitting such as the splitting between ω^+ and ω^- modes predicted at $\theta_R=\pi$ in the triad model. However, in a recent publication, Gullikson *et al.*, by virtue of a many-frequency experiment, have shown that such a splitting is not observed for *Cu*Mn(8 at. %).[7] In addition to this evidence we think that the K values which we have now found show that there is something wrong, and that the validity of the hydrodynamical models for π rotations does not hold. We feel that we have demonstrated here that an approach using only parallel and antiparallel data will lead nowhere. Therefore, let us now look to see if the hydrodynamic approach has any validity for $\theta_R \neq 0$, and, if so, how large θ_R can be for the theories still to hold.

B. Full angle dependence for *Cu*Mn(5 at. %)

We have measured the full angle dependence of the ESR spectrum of *Cu*Mn(5 at. %) in the following way. After field-cooling the sample through T_f in a field $\vec{H}_c$, we removed the field, rotated the sample by θ_H deg, and applied an increasing field to record the resonance. It turned out to be necessary to heat the sample between measurements at different angles θ_H. If we do not heat the sample but simply take measurements at increasing angles, then we find that the shift at 360° is 10% smaller than the one at 0°. We even find that after ZFC there is a clear angular dependence in the spectra, the shift being 650 Oe for 0°, 390 Oe for 180°, and 280 Oe for 360°, whereas there should be no angle dependence at all. This obviously suggests that there is a non-negligible isothermal remanent magnetization (IRM) and isothermal remanent anisotropy (IRA) induced by the measuring field at 9 GHz, and thus a change of the original remanence direction $\hat{N}$. We have therefore always heated the sample in between the angles so as to erase this IRM. Of course, one cannot prevent an IRM component of the total magnetization which is in resonance, but at least this way one makes sure that the total magnetization at one angle θ_H does not contain IRM components induced by measurements at other values of θ_H. We present the measurements in Fig. 4. We have used $\nu=9.44$ GHz and $H_c=12$ kG at $T\approx 3$ K. Also shown are two fits to the hydrodynamic models: The first fit for both models is made using K_1 and K_2 values that were obtained in the way described in the preceding section, i.e., using dc-magnetization data for σ and χ and using only H^0 and H^π from the ESR. Consequently, the theory fits to the experimental points at $\theta_H=0$ and π. One can see that in both models the theoretical fit is rather bad. A maximum in the angle dependence is predicted which is not observed at all; also, the predicted values of H are larger than ω/γ for

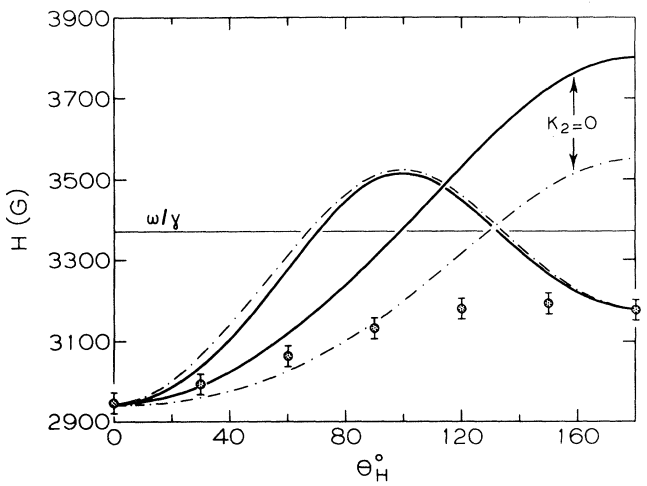

FIG. 4. Resonant field H in G vs angle θ_H in degrees between $\vec{H}$ and the cooling field $\vec{H}_c$ ($H_c=12$ kG) for *Cu*Mn(5 at. %) sphere at $T\approx 3$ K. Circles represent experimental data. Two different sets of fits are shown: The first fit forces points at $\theta_H=0$ and π, and the second fit has $K_2=0$. Solid lines are fits in the vector model, and dashed-dotted lines are for the triad model. Also shown is the line ω/γ ($g=2$). Measuring frequency is 9.44 GHz.

$70°<\theta_H<130°$, but in the experiment all H values are smaller than ω/γ. Clearly, the price that one pays for having the $\theta_H=\pi$ point fit is the loss of all points in between.

The second fit shown in Fig. 4 is one for which we have taken $K^+=K_1$, so that $K_2=0$. The reason for this may not be readily apparent as the dc-magnetization data show that $K_2\approx\frac{1}{2}K_1$ at this temperature. We shall return to this point below. For now, we note that this second fit is really rather better. The vector model fits the data up to $\theta_H=30°$, equivalent to $\theta_R\approx 25°$, whereas the triad model shows a reasonable fit up to $\theta_H\approx 90°$, equivalent to $\theta_R\approx 70°$. Beyond 90°, neither model can fit the data. Again we have a situation where only a limited range of angles can be fitted to the theory, but now at least we have a sound physical reason why this is so: When the rotation angle θ_R becomes too large, rigid spin rotation breaks down and the fit must break down also. (Also, because of the introduction of IRA the original memory direction is lost.) In fact, this method is rather sensitive in determining just where this rigid-rotation breakdown occurs. In this respect the ESR measurements and their interpretation run completely parallel to, e.g., torque measurements and their interpretation.[5]

We now return to the reason for taking $K_2=0$ or at least very small. The argument runs as follows. One supposes that the uniaxial character manifest in the magnetization hysteresis cycles is actually some kind of artifact. Borrowing the terms used by Saslow,[4] we can say that the anisotropy energy is determined by the orientation of the spin triad $\hat{n},\hat{p},\hat{q}$ with respect to the anisotropy triad $\hat{N},\hat{P},\hat{Q}$. If, for large enough negative fields, not only the spin triad but *also* the anisotropy triad reverses, perhaps because the temperature is not low enough, then, upon coming back with the field, the whole situation is mirrored with respect to $H=0$ and reversal of the spin triad will occur at positive fields, showing apparent uniaxial character. In fact, as long as no real large-angle rotations of the spin triad have taken place, no quasiuniaxial character has been induced and one may say that the total anisotropy is purely unidirectional.

IV. CALCULATION OF OSCILLATOR STRENGTH IN THE VECTOR ANISOTROPY MODEL

We have seen so far that some care must be taken when applying the hydrodynamic models in the case when $\theta_R\neq 0$. But how about the case $\theta_R=0$? We have already mentioned in Sec. III that we have identified the mode which is usually observed with ω^+; a clear verification of the validity of either theory would be the observation of an ω^- mode,[14] whereas observation of an ω_L mode supports the triad model. In Ref. (7) the case for the triad model is supported through the observation (for $\theta_R\leq 35°$), of the admixture of an additional mode into the ω^+ mode. We have tried to focus on the ω^- mode (at $\theta_R=0$), which has not been observed yet in pure *Cu*Mn.

Of our three samples, only the 5-at. % sample has a predicted ω^- mode at $\theta_R=0$ in the spectrometer frequency region where we have the best sensitivity, namely between 9 and 10 GHz. Therefore we have taken the 5-at. % sample and searched thoroughly in the region around $H=0$, as indicated in Fig. 3. We were unable to find any indication of a resonance in this region. In order to find a possible explanation for this we have calculated the relative expected intrinsic ESR intensities, in the vector model, the model which was most easily accessible.

We start from the equations of motion

$$\dot{\vec{M}}=\gamma(\vec{M}\times\vec{H})-\gamma K(\hat{N}\times\hat{n})\,, \tag{5}$$

$$\dot{\vec{n}}=\gamma\left[\frac{\vec{M}}{\chi}-\vec{H}\right]\times\hat{n}\,, \tag{6}$$

appropriate to a vector-type free energy with unidirectional anisotropy

$$F=\frac{1}{2\chi}(\vec{M}-\vec{\sigma})^2-\vec{M}\cdot\vec{H}-K(\hat{N}\cdot\hat{n})\,. \tag{7}$$

Linearization is obtained via the substitution

$$\vec{M}=\vec{\sigma}+\chi\vec{H}+e^{j\omega t}\vec{m},\quad \vec{H}=\vec{H}_0+e^{j\omega t}\vec{h},\quad \vec{n}=\vec{N}+e^{j\omega t}\vec{p}\,.$$

An end result of the calculation is

$$\chi(\omega)=\frac{m^+}{h^+}=\chi\frac{(\omega_\sigma+\omega_0)(\omega-\omega_\sigma)-\omega_A^2}{(\omega+\omega_0)(\omega-\omega_\sigma)-\omega_A^2}\,, \tag{8}$$

where $m^+=m_x+jm_y$, $h^+=h_x+jh_y$,

$$\omega_\sigma=\gamma\sigma/\chi,\quad \omega_0=\gamma H_0,\quad \omega_A^2=\gamma^2K/\chi\,.$$

The resonance frequencies can be found by setting the denominator to zero, and one finds

$$\omega_0^-=-\omega+\frac{\omega_A^2}{\omega-\omega_\sigma}\,, \tag{9}$$

or, expressed in H,

$$H_{\rm res}^{-}=-(\omega/\gamma)+\frac{K}{\chi(\omega/\gamma)-\sigma}\ , \tag{10}$$

which is the usual form in the vector model (res denoting resonance). The other root $H_{\rm res}^{+}$ is found if in the original microwave field the opposite polarization $\vec{h}e^{-j\omega t}$ is also considered, in which case

$$\frac{m^{+}}{h^{+}}=\chi\frac{(\omega_\sigma+\omega_0)(-\omega-\omega_\sigma)-\omega_A^2}{(-\omega+\omega_0)(-\omega-\omega_\sigma)-\omega_A^2}\ , \tag{11}$$

obtained by setting $\omega\rightarrow-\omega$. Now setting the denominator to zero yields

$$\omega_0^{+}=\omega-\frac{\omega_A^2}{\omega+\omega_\sigma} \tag{12}$$

or

$$H_{\rm res}^{+}=(\omega/\gamma)-\frac{K}{\chi(\omega/\gamma)+\sigma}\ . \tag{13}$$

Here we use $\omega_0=\gamma H$, where H is the variable field and ω is the fixed measuring frequency. Expressions (8) and (11) can be combined as

$$\frac{m^{+}}{h^{+}}=\frac{\alpha(H_{\rm res}^{+})}{H-H_{\rm res}^{+}}+\frac{\beta(H_{\rm res}^{-})}{H-H_{\rm res}^{-}}\ , \tag{14}$$

where $\alpha(H_{\rm res}^{+})$ and $\beta(H_{\rm res}^{-})$ are now the oscillator strengths of the $+$ and $-$ modes, respectively. The oscillator strength thus provides a measure for the intensity of the resonant signal because the apparent divergences at $H=H_{\rm res}^{\pm}$ are, of course, resolved as soon as dissipation is included in the equations of motion. We find

$$\alpha(\omega_0^{+})=\omega_\sigma+\omega_0^{+}+\frac{\omega_A^2}{\omega+\omega_\sigma}=\omega_\sigma+\omega \tag{15}$$

or

$$\alpha(H_{\rm res}^{+})=\sigma+\chi H_{\rm res}^{+}+\frac{K}{(\omega/\gamma)+\sigma/\chi}=\sigma+\chi(\omega/\gamma)\ , \tag{16}$$

and

$$\beta(\omega_0^{-})=\omega_\sigma+\omega_0^{-}-\frac{\omega_A^2}{\omega-\omega_\sigma}=\omega_\sigma-\omega \tag{17}$$

or

$$\beta(H_{\rm res}^{-})=\sigma+\chi H_{\rm res}^{-}-\frac{K}{(\omega/\gamma)-\sigma/\chi}=\sigma-\chi(\omega/\gamma)\ . \tag{18}$$

A simple check of our calculation is the paramagnetic regime: For $K\rightarrow0$ and $\sigma\rightarrow0$ the oscillator strengths become $\chi\omega_0$, in agreement with well-known theory. The next simplest check is the spin-glass regime after ZFC ($\sigma=0$). Since K does not enter into the determination of α and β, the ratio between α, at a frequency ω_1 where the ω^{+} mode can be observed, and β, at a frequency ω_2 where the ω^{-} would be observed, would be ω_1/ω_2. In ZFC conditions, $\omega_2<\omega_1$, and for our experiments, $2<\omega_1/\omega_2<10$. This certainly does not explain nonappearance of the ω^{-} mode, e.g., at 4 GHz (cf. Fig. 2 of Ref. 9). These expressions are valid for the case where the experiment is done in the usual way, i.e., when the measuring frequency ω is kept constant and the field H is varied to record the resonance. In the case when H is kept constant and ω is varied, expressions (9) and (12) should be used without the transformation to fields. For the FC condition shown in Fig. 3, we find, at $T\approx3$ K for the 5-at. % sample, where $(\omega/\gamma)=3369$ G, $K=3230$ erg/cm^3, $\sigma=3.54$ G, and $\chi=13.4\times10^{-4}$, that

$$H_{\rm res}^{+}=2969,\quad \alpha(2969)=8.05\ ,$$

$$H_{\rm res}^{-}=-50,\quad \beta(-50)=-0.97\ .$$

Again, the $|\alpha/\beta|$ ratio of 8 does not explain nonobservation of the ω^{-} mode: However, there are two other factors which play a role here.

(1) The slope in the ω-vs-H diagram for FC in 12 kG is smaller by a factor of 3 for the ω^{-} mode; in the measured derivative spectrum this slope appears squared. This gives an additional factor of 10.

(2) The relaxations of the modes may not be the same. From intensity considerations, that is nonobservation of the ω^{-} mode, we would expect it to have a relaxation at least 3 times larger than the ω^{+} mode. From these FC and ZFC cases it would seem as if a larger relaxation of the ω^{-} mode is the main reason for nonobservation, unless other considerations come into play.

V. CONCLUSIONS

We have measured the ESR ω-vs-H diagrams for *Cu* with 2- to 5-at. % Mn alloys both when $\vec{H}$ is parallel and antiparallel to $\vec{H}_c$ (the cooling field). These diagrams can be explained by the hydrodynamic theories with the anisotropy K_1 and K_2 (see Table I) as parameters. When the dc magnetization is used to determine K_1 and K_2 independently, values are found which are not consistent with those found from the ESR. This inconsistency implies that the assumption of rigid rotations may not be valid across the entire range 0°–180°.

In order to examine the applicability of these models more closely we have measured the full angle dependence for the 5-at. %Mn sample. This angle dependence is best described by the triad model using $K_2=0$ and we can obtain a limited fit to the data for small θ_R angles ($\lesssim70°$). The present set of experimental data is consistent with the results of previously published experiments.[1,7,12] We attribute the breakdown of the fit beyond 70° to nonrigid spin rotations.

We have calculated the oscillator strength of the predicted ω^{+} and ω^{-} resonance modes in the vector model. Our calculations show a reduced peak-to-peak amplitude of the first-derivative ESR spectrum (~100) to be observed for the ω^{-} mode. However, this factor can easily be overcome in the experimental situation and thus oscillator-strength considerations do not fully explain why

an ω^- resonance was not observed. The linewidth calculations of Monod[15] may shed more light on this question.

In conclusion, dynamical experiments on spin-glasses indicate that only for small deviations from equilibrium does the spin system behave as a rigid body. This means that hydrodynamic theories can only be used to describe these phenomena at small angles between $\vec{H}$ and $\vec{H}_c$. The results of an ESR investigation of the full angle dependence on higher-concentration ($\sim$20-at. %Mn) *Cu*Mn alloys will shortly be forthcoming.[16]

ACKNOWLEDGMENTS

We wish to thank J. A. Mydosh for valuable discussions and M. Zomack for his assistence in performing the 1-, 3-, and 4-GHz experiments at Freien Universität Berlin. This work was supported by the Nederlandse Stichting voor Fundamenteel Onderzoek der Materie (FOM), the Deutsche Forschungsgemeinschaft, Sonderforschungsbereich 161, and, in part, by the National Science Foundation—Condensed Matter Theory Program Grant No. DMR-81-20827.

[1]S. Schultz, E. M. Gullikson, D. R. Fredkin, and M. Tovar, Phys. Rev. Lett. 45, 1508 (1980).

[2]T. Iwata, K. Kai, T. Nakamichi, and M. Yamamoto, J. Phys. Soc. Jpn. 28, 582 (1970).

[3]C. L. Henley, H. Sompolinsky, and B. I. Halperin, Phys. Rev. B 25, 5849 (1982).

[4]W. M. Saslow, Phys. Rev. Lett. 48, 505 (1982); Phys. Rev. B 26, 1483 (1982).

[5]A. Fert and F. Hippert, Phys. Rev. Lett. 49, 1508 (1982).

[6]H. Alloul and F. Hippert, J. Magn. Magn. Mater 31-34, 1321 (1983).

[7]E. M. Gullikson, D. R. Fredkin, and S. Schultz, Phys. Rev. Lett. 50, 537 (1983).

[8]From recent susceptibility measurements it is clear that correlations between the spins exist even up to $T=5T_f$. See, e.g., A. F. J. Morgownik and J. A. Mydosh, Phys. Rev. B 24, 5277 (1981). However, we verified that in the ESR it was not necessary to heat up to more than $2T_f$.

[9]F. R. Hoekstra, K. Baberschke, M. Zomack, and J. A. Mydosh, Solid State Commun. 43, 109 (1982).

[10]The 9-GHz measurements were all performed in an electromagnet where the remanence was smaller than 5 G.

[11]For a review, see P. M. Levy, C. Morgan-Pond, and A. Fert, J. Appl. Phys. 53, 2168 (1982).

[12]See Ref. 1 and also J. S. Kouvel, J. Phys. Chem. Solids 21, 57 (1961); F. Hippert, H. Alloul, and J. J. Préjean, Physica 107B, 645 (1981); F. Hippert, H. Alloul, and A. Fert, J. Appl. Phys. 53, 7702 (1982).

[13]The reason for not taking $\nu=4.03$ GHz as a reference frequency for the 3.5-at. % probe is that near this frequency Eq. (4) diverges, corresponding to the fact that the splitting between ω^+ and ω^- in the triad model occurs just there.

[14]There is some confusion about the notation of ω^+ and ω^- modes. It does not seem to be very useful to use strictly the sign of the roots as labels. It would be more physical to label those resonances which are close to $g=2$ for large fields ω^+ and the other modes ω^-. This means that we would also label ω^+ the resonances at negative fields in Figs. 1—3, where the more interesting mode to be detected is the other branch, namely ω^-.

[15]P. Monod (private communication).

[16]F. R. Hoekstra, G. J. Nieuwenhuys, and J. A. Mydosh (unpublished).